Thin Solid Films 531 (2013) 340–348

Contents lists available at SciVerse ScienceDirect

Thin Solid Films

journal homepage: www.elsevier.com/locate/tsf

Quantitative analysis of the mechanical robustness of multilayered bonding pad on a semiconductor device by nanoindentation and nanoscratch tests

Dong Kil Shin [*], Jay Im

Department of Mechanical Engineering, Korea Advanced Institute of Science and Technology (KAIST) 291 Daehak-ro, Yuseong-gu, Daejon 305-701, Republic of Korea

ARTICLE INFO

Article history:
Received 9 May 2012
Received in revised form 14 December 2012
Accepted 18 December 2012
Available online 6 January 2013

Keywords:
Multilayered bonding pad
Nanoscratch test
Nanoindentation test
Semiconductor device
Wirebonding
Pad damage

ABSTRACT

Mechanical robustness of a bonding pad on an electronic device, consisting of the top aluminum layer, 40 nm thick intermediate titanium nitride (TiN) barrier layer, and 350 nm thick bottom aluminum layer, was investigated with respect to the thickness of top aluminum layer ranging from 250 nm to 650 nm. Mechanical responses of the pad were evaluated using wire pull test, nanoindentation test, and nanoscratch test. The bonding quality was degraded with the decreasing thickness of top aluminum layer, due to the increasing risk of mechanical damage of this layer and the breakage of the underlying TiN layer. The apparent elastic modulus of the thinner pad increased faster than that of the thicker one as a function of indentation depth. Apparent friction coefficient exhibited a complex, yet understandable, pattern amenable to the relative difficulty of the scratch tip traveling through the three layers in the pad assembly. The breakage of TiN caused an abrupt drop in the load vs. penetration curves in the nanoscratch test, the coincidence of which was verified by subsequent cross-sectional analysis. The longitudinal scratch distance to the TiN breakage can serve as a useful parameter to qualify the mechanical stability of the bonding pad.

1. Introduction

Thin layers on semiconductor devices are composed of various materials and structures. Bonding pad is exposed on the surface of the semiconductor device and is an important connection site between the silicon device and the first-level electronic package. On the pads, both chemical loading and mechanical loading are applied, where the former is induced by wafer fabrication process such as passivation layer opening, dielectric layer opening, and surface cleaning while the latter is induced by subsequent electrical testing and packaging processes. Therefore, the pads need to be built strong enough to endure these external loads [1].

Advanced devices are invariably seen to possess mechanically weak pad structure and materials. In order to complement the weakness, the capability of wire bonding machine has been improved for decades, accompanying with the development of new wire materials and optimization of the wire bonding process involving bonding force, power, time, and so on [2,3]. In-plane pad design or 3D vertical structure of bonding pad has been optimized to relieve stress concentration and to prevent such pad failures as cratering, lifting, etc. [4].

On the pad, the outermost metal layer is crucial for the robustness of the pad. In the electrical test process, the contact force of the test probe is large enough to leave a deep trace on the metal. In the wire bonding process, a combination of mechanical loadings – compression, shear, high speed impact force, and high frequency ultrasonic vibration force – is applied to the pad, resulting in damage in and on the pad [5]. In addition, the pad metal interacts with the gold wire and forms intermetallic compounds (IMCs) with time. The metal should be in sufficient volume to obtain an evenly distributed IMC [6].

Therefore, it is important to understand the effect of metal thickness on the bondability and mechanical response of the pads resulting from the wire bonding process. Wire pull test and ball shear test have been widely used for the evaluation of bonding quality [7–9]. However, these tests are insufficient to quantitatively assess the bondability. In order to establish a design guide and to achieve an optimum design, the failure mechanism and the corresponding key parameters should be verified. Furthermore, elasto-plastic properties of the pad metal layer and brittle fracture of the underlying layer should be investigated, and the mechanical responses should be measured quantitatively. Instrumented indentation and scratch test are useful methods to undertake these tasks [10,11].

If only the pad layers are considered, they consist of a typical tri-layer structure obtained by sequentially depositing aluminum, titanium nitride (TiN), and aluminum. In other words, a hard thin TiN layer is embedded between two thicker ductile aluminum layers. Scratch test on such ductile metal is useful to investigate plastic properties and friction coefficient of the thin metal film. The plasticity of ductile metal resulted in deep groove and debris in front of and both sides of the scratch tip [12]. The plastic properties of the material could be achieved by forward or reverse algorithms [13]. The stress concentrations in front of and under the tip and damage evolution of ductile metal could be verified by finite element analysis [14].

---

[*] Corresponding author. Tel.: +82 42 350 5294.
E-mail address: dk.shin@kaist.ac.kr (D.K. Shin).

0040-6090/$ – see front matter © 2013 Elsevier B.V. All rights reserved.
http://dx.doi.org/10.1016/j.tsf.2012.12.088

Middle TiN and bottom aluminum make a typical structure composed of a hard coating and soft substrate. This kind of film has been studied from various points of view of tribology, wear, adhesion, and so on [15–20]. Failure modes of hard coating were varied depending on the material properties of the films, shape of the scratch tip, and friction between the tip and the surface [21].

However, a tri-layer combination as in this study, soft/hard/soft, has not been studied extensively. Therefore, we employed nanoindentation and nanoscratch techniques to investigate the mechanical behavior of bonding pad followed by post-mortem cross-sectional analysis. Bondability was evaluated by wire pull test.

2. Characteristics of aluminum metal layer as a function of metal thickness

Aluminum metallization bonding pad was investigated in this study. Fig. 1(a) shows the top view of 80 μm × 80 μm bonding pad assembly. The probe mark shown on the pad was induced by scratch mode of a test probe during the wafer test process. In most cases, wires are bonded on the pads already probed, although bonding on non-probed pad is sometimes practiced. Fig. 1(b) shows a schematic of the vertical structure of the bonding pad. On the 2800 nm thick silicon oxide layer, TiN (20 nm) and Ti (<10 nm) were deposited, and the first aluminum metal layer (M1) of 350 nm was deposited. On top of the M1 layer, Ti (<10 nm)/TiN (40 nm)/Ti (<10 nm) was deposited sequentially. Then the second aluminum metal (M2) was deposited. Note that the deposited titanium reacts with the aluminum to produce TiAl IMC [1]. Silicon nitride passivation was deposited on the M2 layer and polyimide was coated on the passivation layer. Finally, bonding pad and fuse area were opened by a chemical etching process. During the etching process, the upper side of the M2 was also etched to some degree; hence a thinner M2 layer than the original was remained.

In this study, five cases of final M2 thickness, 250 nm, 330 nm, 450 nm, 550 nm, and 650 nm, were considered. The final M2 thickness resulted after pad opening and etching process of the surface of the initially thicker M2. Other than the M2 thickness, all other processes were kept the same for all cases so that the bulk properties and surface conditions of M2 remained essentially unchanged. Gold wire, 25.4 μm in diameter, was bonded to the pad using a thermo-sonic ball bonder, which was set at 150 °C and the vibration frequency of 120 kHz.

Characteristics of the wire bonding were examined by a wire pull test (Dage Co.) at room temperature for 224 wires for each M2 thickness case. In order to accelerate the IMC growth and damage evolution, the samples were aged for 3 h at 200 °C. Then, wire pull test was performed to evaluate the bondability. In general, failure modes of the wire pull test are reported to be as follows; cratering under the bonding pad, lift off of bonding pad metallization, ball lift, ball neck break, mid span wire break, and heel break on printed circuit board [1]. The failure modes observed in this study were ball neck failure, metal lift, and ball lift. Fig. 2 shows typical failure modes of the metal lift and ball lift.

Because metal lift and ball lift were not easily distinguishable by naked eyes, the sum of both occurrences was considered instead as shown in Fig. 3. When the M2 thickness was 650 nm, there was no metal lift or ball lift, but all failures were by ball neck break. However, the ratio of the metal lift or ball lift to the entire failure modes started to increase with decreasing M2 thickness, and it was dramatically increased to 14% when the M2 metal thickness reduced to 250 nm.

Wire bonded pad was sectioned and observed by focused ion beam (FIB) at an acceleration voltage of 50.0 kV (Micrion 9500, FEI/Micrion Co.). Fig. 4 shows cross sectional views of the wire bonded pad prior to thermal aging. The grain size at the bottom portion of gold was seen smaller than that of the upper portion, indicating that the bottom portion of gold was more severely deformed by shear and compression forces of capillary. Fig. 4(a) shows the case of 250 nm M2, where the white layer between gold and aluminum is AuAl IMC layer. At the center of the interface, indicated as C250 in the figure, it is observed that most of M2 was consumed by IMC formation and other remaining M2 was distributed with an uneven thickness. Besides, the M1 layer also shows a wavy pattern, which could result from both vibration of capillary during wire bonding and the scratch of wafer test probe prior to wire bonding as has been shown in Fig. 1(a). The edge side of the bonding area, E250, also shows a wavy pattern and an uneven thickness of M1. Furthermore, two places of broken TiN are observed.

When M2 is of intermediate thickness, 330 nm, a thin and unstable M2 layer is still seen as shown in E330 of Fig. 4(b). But the M1 layer is stable and the TiN layer is intact without breakage. For the case of 550 nm at the edge side, E550, in Fig. 4(c), the M2 layer largely remains with a relatively uniform thickness distribution, and there is no TiN breakage.

Long term characteristics of the interface were examined by aging the sample at high temperature. Wirebonded samples, without epoxy molding compound applied, were stored at 200 °C chamber for 20 h to accelerate the IMC formation. Fig. 5 shows typical cross-sectional views of the pad near the outer edge of the ball boundary as marked in the inset of Fig. 5(a).

As shown in Fig. 5(a) for M2 of 250 nm, there is gold-rich IMC on aluminum-rich IMC in M2 layer. Through the broken TiN cleavage, gold penetrated into the M1 and AuAl IMC was also formed in the M1 layer. The volume of the IMC was larger than the sum of each constituent material [22], so the IMC in M1 layer pushed the TiN upward and broke another site of TiN layer. The image for M2 of 330 nm in

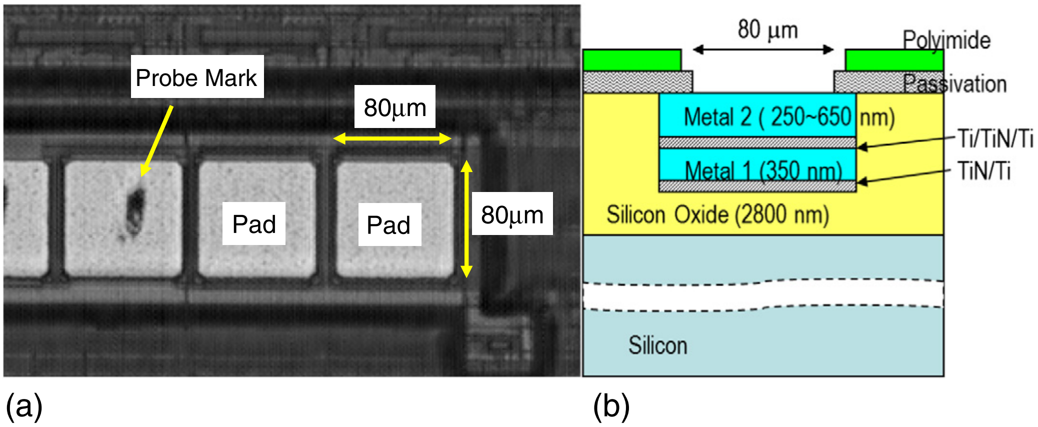

Fig. 1. (a) Aluminum bonding pads on a chip and (b) schematic of vertical structure of the bonding pad.